



ELSEVIER

Journal of Nuclear Materials 283–287 (2000) 1306–1310

journal of  
nuclear  
materials

www.elsevier.nl/locate/jnucmat

# A microstructural study of the oxide scale formation on ODS Fe–13Cr steel

D.T. Hoelzer<sup>\*</sup>, B.A. Pint, I.G. Wright

*Oak Ridge National Laboratory, P.O. Box 2008, Bldg. 5500, Oak Ridge, TN 37831-6376, USA*

## Abstract

The high-temperature oxidation behavior of a  $Y_2O_3$ -dispersed Fe–13Cr steel was investigated in air at temperatures of 700°C, 800°C, and 900°C for 10 000 h. The kinetic data showed that oxide scale formation obeyed a parabolic rate law at each temperature and that the oxidation rate was lower than in other studies based on shorter test times. Microstructural analysis of the oxide scales formed at 700°C and 800°C was conducted using cross-sectional specimens and analytical electron microscopy (AEM). This analysis showed that the main scale was a continuous Cr-oxide and that an underlying amorphous silica layer formed at both temperatures, despite the low Si content (0.05 wt%) in the alloy. © 2000 Elsevier Science B.V. All rights reserved.

## 1. Introduction

Ferritic steels are being considered for structural applications in fusion energy systems because of their reduced activation and excellent resistance to void swelling. Advances in developing improved properties of these steels have been made using oxide dispersion strengthening (ODS). The ODS approach has been shown to improve the high-temperature mechanical strength of ferritic steels while maintaining acceptable low-temperature toughness. The development goal for ODS ferritic steels is to increase the temperature limit for use from approximately 550°C to >650°C. However, an issue in the application of ODS ferritic steels at higher temperatures is their oxidation behavior, especially for applications in gas–metal environments. The purpose of this study was to investigate the oxidation behavior of an ODS Fe–13Cr steel in air at temperatures being considered for their application.

## 2. Experimental

The ODS Fe–Cr steel used in this study was developed and fabricated in a joint program between Kobe Steel and Sumitomo Metal Industries of Japan [1], and its composition is shown in Table 1. Specimens were prepared as  $\sim 1.2 \text{ cm} \times 1.7 \text{ cm} \times 0.1 \text{ cm}$  thick coupons from the as-supplied rod; the specimen surfaces were polished to 0.3  $\mu\text{m}$  alumina and ultrasonically cleaned in acetone followed by cleaning in high-purity methanol prior to oxidation. The oxidation exposures were conducted in 1 atm of laboratory air at 700°C, 800°C, and 900°C for 10 000 h with specimens held in individual, lidded, pre-annealed alumina crucibles to allow the total oxygen uptake to be measured and to catch any spalled oxides. Mass gain of the coupons was measured discontinuously at 500 h intervals using a Mettler AG245 microbalance.

After oxidation, the specimens were examined by both scanning electron microscopy (SEM) and cross-section metallography. Specimens were also sectioned perpendicular to the steel–oxide interface and prepared as cross-sectional thin foils. A layer of Cu was electrochemically deposited on the cross-sectioned samples, and then they were thinned by mechanical dimpling and ion milling techniques. The thin foil samples were examined by transmission electron microscopy (TEM) using a Philips CM12 fitted with an X-ray energy dispersive spectrometer (XEDS).

<sup>\*</sup> Corresponding author. Tel.: +1-865 574 5096; fax: +1-865 574 0641.

*E-mail address:* hoelzerd@ornl.gov (D.T. Hoelzer).

Table 1  
Composition of the ODS Fe–Cr steel

Element	wt%	at.%
Fe	83.04	83.13
Cr	13.16	14.15
W	2.80	0.85
Ti	0.32	0.37
Si	0.05	0.10
S	0.007	0.011
C	0.05	0.23
Y <sub>2</sub> O <sub>3</sub>	0.241	0.298
Others	0.332	0.0861

### 3. Results

#### 3.1. Oxidation kinetics

Fig. 1 shows the total (specimen + spalled scale) and specimen-only mass gains measured at each oxidation temperature. The data are plotted as mass gain vs square root of time, and indicate that the oxidation closely followed a parabolic rate law at each temperature. Oxidation at 700°C and 800°C resulted in very low mass gains. At 900°C, the large difference between total mass gain and specimen mass gain was due to evaporation of CrO<sub>3</sub>, which was redeposited on the walls of the alumina crucible. There was no spalled oxide at any temperature. Parabolic rate constants derived from the kinetic curves were 1.9, 71, and 630 ( $\times 10^{-16}$  g<sup>2</sup> cm<sup>-4</sup> s<sup>-1</sup>) at 700°C, 800°C, and 900°C, respectively. For comparison [2], the parabolic rate constant for a relatively pure Fe–25 wt%Cr alloy oxidized in air at 700°C (though for only 100 h) was  $370 \times 10^{-16}$  g<sup>2</sup> cm<sup>-4</sup> s<sup>-1</sup>. Although this alloy developed a Cr-rich oxide scale, its rate constant at 700°C was some 200 times larger than for the ODS Fe–13Cr alloy. The value of the activation energy of the

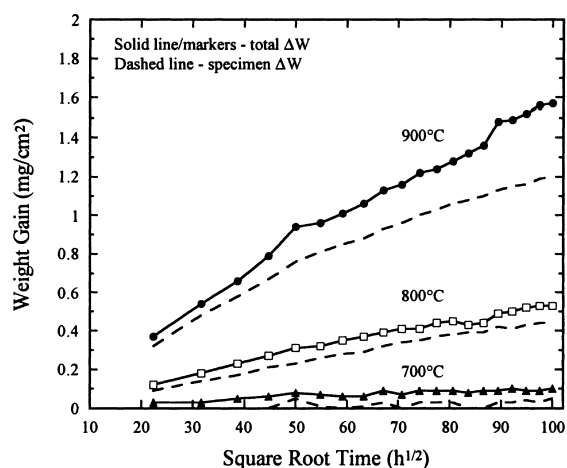


Fig. 1. Weight gains measured from specimens that were oxidized at high temperatures for 10 000 h.

process controlling the rate of oxidation, obtained from a simple Arrhenius plot of the data, was 66 kcal/mol.

#### 3.2. Microstructural analysis

The matrices of the ODS ferritic steel specimens and the surface scales that formed on them during oxidation at 700°C and 800°C were characterized in detail; however, at the time of reporting, the 900°C specimen was not ready for characterization. Fig. 2 shows representative images of the surface scales obtained by light microscopy. In general, the scales were  $<1$   $\mu$ m thick at 700°C and  $<5$   $\mu$ m thick at 800°C and were adherent to the steel. Both temperatures resulted in scales having fairly rough surfaces with relatively uniform thicknesses. TEM analysis of the specimens after oxidation showed matrices that consisted of elongated grains that were  $<0.5$   $\mu$ m wide and several microns long, complex Y/Ti-oxides that were  $<20$  nm in size dispersed along grain boundaries and in the matrix, and an inhomogeneous distribution of carbides and non-yttria containing oxides that were usually  $>1.0$   $\mu$ m in size.

The typical scale morphology observed on the oxidized specimens consisted of surface Cr-rich oxide grains that were separated from the ferritic steel by an Si-oxide layer. TEM micrographs showing the typical scale cross-sections observed in the 700°C and 800°C specimens are presented in Fig. 3. At both temperatures, the Si-oxide layer was nearly continuous, but areas of contact still existed between the Cr-oxide surface scale and steel. In

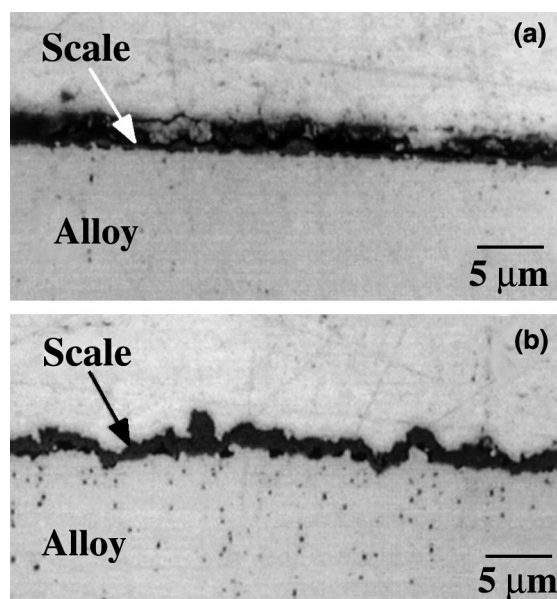


Fig. 2. Light micrographs of the surface scales that formed on the ODS ferritic alloy during oxidation in air at (a) 700°C; (b) 800°C.

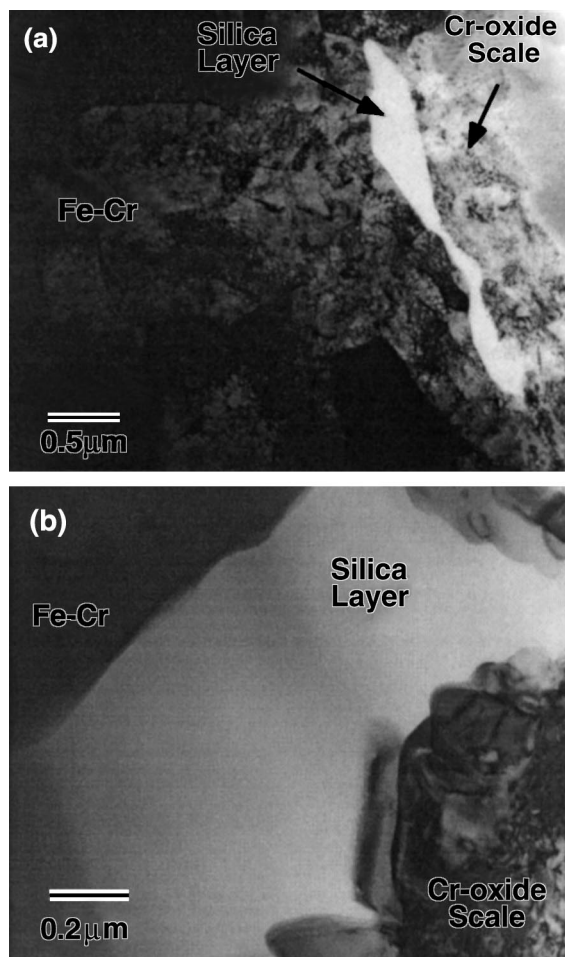


Fig. 3. TEM micrographs of the surface scales that formed on the ODS ferritic alloy during oxidation in air at (a) 700°C; (b) 800°C.

general, the thickness of the Si-oxide layer depended upon the oxidation temperature, but it was non-uniform in thickness. At 700°C, the layers were  $\sim 0.3$  and  $\sim 0.9$   $\mu\text{m}$  at 800°C. The Si-oxide layer was determined by convergent beam electron diffraction (CBED) to have an amorphous structure and by XEDS to contain essentially only silicon and oxygen, which was consistent with the  $\text{SiO}_2$  (silica) phase. These results are shown in Fig. 4 for a representative silica layer observed in the 800°C oxidized sample.

The Cr-oxide surface scale that formed at 700°C consisted of small grains throughout the scale thickness. The grain size was determined from those that were oriented near Laue conditions in bright-field images and was found to be less than  $\sim 200$  nm. Voids and second-phase particles were not observed in the scale microstructure. Fig. 5 shows representative XEDS spectra and the selected area electron diffraction (SAED) pattern of

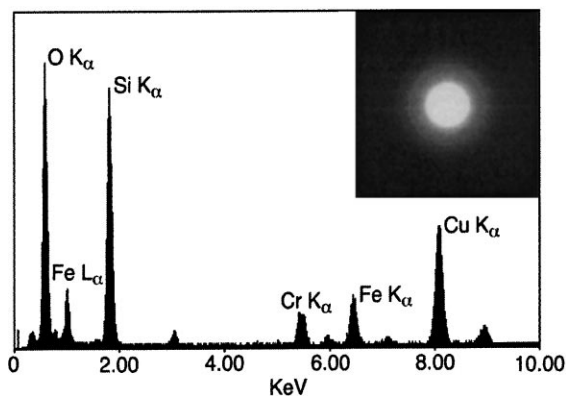


Fig. 4. Compositional (XEDS spectra) and structural analysis (CBED insert) of the silica layer that formed on the ODS ferritic alloy at 700°C and 800°C.

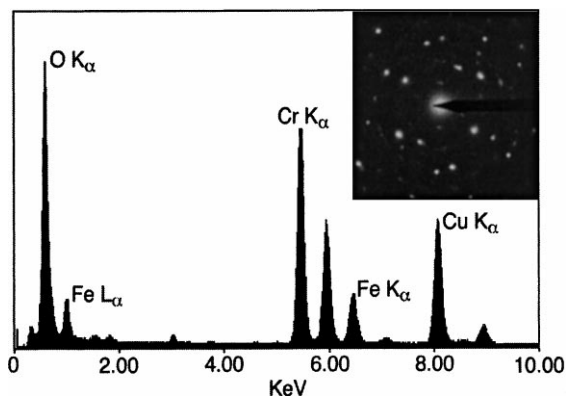


Fig. 5. Compositional (XEDS spectra) and structural analysis (SAED insert) of the  $(\text{Fe,Cr})_3\text{O}_4$  spinel phase that formed on the ODS ferritic alloy at 700°C.

the scale. The chemical analysis indicated that a limited amount of Fe was present in the Cr-rich oxide scale. The diffraction pattern shown in the inset was obtained using a small SAED aperture to emphasize the polycrystalline microstructure. The structural analysis was based on the measurements of both diffraction spots and diffuse partial rings observed in the SAED pattern and showed that the predominant crystal structure of the grains was consistent with the  $(\text{Fe,Cr})_3\text{O}_4$  spinel phase (PDF #12-0559).

At 800°C, the surface scale formed with both small and large Cr-oxide grains. The small grains were typically 100 nm in size and formed near the Cr-oxide and silica interface, as shown in Fig. 3(b). Near the gas-surface interface, the Cr-oxide grains were much larger, some  $\sim 2$   $\mu\text{m}$  or larger, and closer in shape to equiaxed rather than columnar. Fig. 6 shows the results of compositional and structural analyses of the oxide scale that

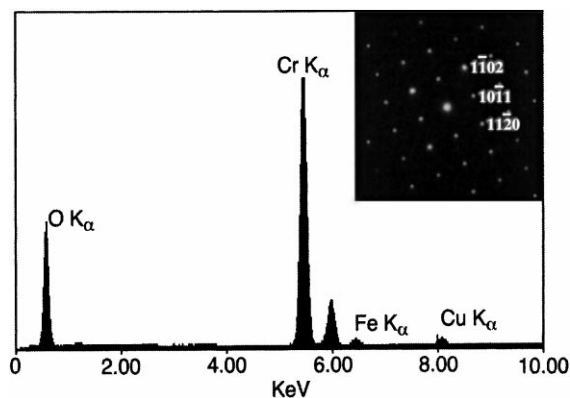


Fig. 6. Compositional (XEDS spectra) and structural analysis (SAED insert) showing the  $[01\bar{1}1]$  zone axis of the  $\text{Cr}_2\text{O}_3$  (chromia) phase that formed on the ODS ferritic alloy at  $800^\circ\text{C}$ .

formed at  $800^\circ\text{C}$ . The large oxides were mostly Cr, and the crystal structure of the Cr-oxide grains was consistent with the  $\text{Cr}_2\text{O}_3$  (chromia) phase (PDF #38-1479) as indicated by the SAED pattern inset, which shows the  $[01\bar{1}1]$  zone axis. Small particle inclusions were also observed in the chromia grains near the silica layer. These particles often contained Fe and Ta along with the Cr from the oxide grains. These particles were believed to be oxides, but further work is needed in order to confirm their crystal structure. No other particles or voids were observed in the Cr-oxide surface scale.

#### 4. Discussion

The excellent oxidation behavior of the ODS Fe–Cr steel cannot be attributed solely to the formation of a continuous Cr-oxide surface scale at all temperatures, since the oxidation rates appear to be significantly slower than expected for rate control by a chromia scale. This result is important since the nominal 13 wt% Cr content in the ODS Fe–Cr steel is near the minimum Cr content required to form a continuous protective scale. It is likely that other contributing factors helped to establish the Cr-oxide scale.

Two possible factors at  $700^\circ\text{C}$  and  $800^\circ\text{C}$  are the  $\text{Y}_2\text{O}_3$  (yttria) dispersion and the silica layer that formed underneath the chromia. Yttria is used because it is thermodynamically stable, and a dispersion of small stable particles reduces the grain size of the Fe–Cr steel. Fine alloy grain size increases the transport of Cr by grain boundary diffusion, allowing rapid diffusion of Cr (and possibly other elements) to the surface, where it can react with O to form the Cr-oxide scale in spite of the low Cr concentration in the alloy. The observation of a semi-continuous layer of silica at the base of the Cr-rich scale suggests the possibility that it acts as a diffusion

barrier to the inward migration of O and outward migration of metallic elements. Previous studies have reported that the formation of a continuous silica scale at the chromia scale–metal interface improved the high-temperature oxidation resistance of stainless steels and higher-Cr containing Fe–Ni–Cr alloys [2–6].

In this alloy, although the silica layers that formed at  $700^\circ\text{C}$  and  $800^\circ\text{C}$  were not continuous and there was no indication, from the oxidation kinetics, of the point at which there was a sufficient volume fraction of silica particles at the alloy–scale interface to affect growth, the non-continuous silica layers appear to have been very effective. However, areas of contact between the Cr-oxide scale and metal would be expected to continue to provide pathways for either O or Cr transport. In the former case, oxide formation would undercut the silica layer while, in the later case, oxide formation would cause a bulge on the surface. However, neither type of feature was observed on these specimens. McDowell and Basu [5] concluded in their study that chromia formed within microcracks in the silica layer, producing diffusion pathways for the rapid outward flux of Cr to the surface. The areas of contact observed in this study are analogous to these microcracks, so that it is suggested that the silica layer effectively limited the kinetics of scale formation by restricting the flux of Cr through the regions of contact between the Cr-oxide and alloy substrate.

The formation of a silica layer was surprising since the  $\sim 0.1$  at.% Si content of the ODS Fe–Cr steel is very low. The Si levels required to form continuous silica layers on stainless steels are reportedly  $\sim 1.1$  at.% Si in Fe–20Cr–25Ni–Nb [6], and  $\sim 2.9$  at.% Si in Fe–18Cr–20Ni [4]. A  $1\ \mu\text{m}$  thick coating of Si preformed on Fe–18Cr–20Ni by chemical vapor deposition also led to the development of a silica sublayer [5]. However, at the temperatures of interest, the rate of diffusion of chromium in the austenitic alloys is some two orders of magnitude slower than in the equivalent ferritic alloys. By extension, it is possible that the rate of diffusion of silicon in the austenitic alloys is significantly slower than in a ferritic matrix, thereby requiring more Si in the alloy to form a silica scale.

The kinetics of formation of a silica layer on the ODS Fe–Cr steel were estimated using the diffusivity data of Ahmad et al. [7], who determined the diffusion rate of Si in Fe–2.25Cr–1Mo ferritic steel (wt%) over the appropriate temperature range. Extrapolation to 10 000 h indicated that the diffusion range for Si was  $\sim 29\ \mu\text{m}$  at  $700^\circ\text{C}$  and  $\sim 50\ \mu\text{m}$  at  $800^\circ\text{C}$ . These values are sufficient to account for the mass transport of Si to the metal surface by normal bulk diffusion processes in this alloy.

A further scenario is that protective scale formation on this alloy was promoted by synergistic action of the  $\text{Y}_2\text{O}_3$  dispersion with Si. If the stabilization of a fine grain size in the alloy by the  $\text{Y}_2\text{O}_3$  resulted in the rapid

formation of a protective Cr-rich outer scale, the consequent maintenance of a low oxygen partial pressure at the scale–alloy interface would favor diffusion of Si from the alloy to the interface. Higher interfacial oxygen partial pressures that would have prevailed in the presence of an Fe-rich outer scale would have resulted in a steeper oxygen concentration gradient in the alloy, favoring internal oxidation of the Si to form discrete precipitates remote from the interface.

The addition of elemental yttrium has been widely used to improve the oxidation resistance of high-temperature alloys [8]. However, the beneficial effect of Y on scale formation is typically observed at temperatures higher than  $\sim 900^\circ\text{C}$  since the diffusivity of Y is very low below this temperature [9]. The results of this study support this general rule since little or no Y was observed in the scale. It is possible that a small amount of Y had segregated to grain boundaries in the Cr-oxide scale, since no voids were observed near the metal–scale interface; previous studies have shown that Y segregation to grain boundaries reduced void formation near the metal–scale interface [9,10]. Since Y could not be detected with statistical significance over the background in XEDS spectra, the suspected enrichment levels for Y segregation must be very low. Further work is planned using a field-emission gun TEM coupled with spectrum imaging to investigate the possibility of Y segregation.

## 5. Conclusions

The oxidation in air of a  $\text{Y}_2\text{O}_3$ -dispersed Fe–13Cr steel resulted in continuous, protective scales at  $700^\circ\text{C}$ ,  $800^\circ\text{C}$ , and  $900^\circ\text{C}$  that formed according to parabolic rate laws at all temperatures. At the gas–metal interface, the scales consisted of  $(\text{Fe,Cr})_3\text{O}_4$  at  $700^\circ\text{C}$  and  $\text{Cr}_2\text{O}_3$  at  $800^\circ\text{C}$ , but there was a non-continuous silica layer between the Cr-oxide scale–metal interface. The formation of the protective scales is attributed to formation of the silica layer, which acted as a diffusion barrier to diffusing

anions and cations, and the contact areas between the Cr-oxides and metal, which acted as diffusion pathways for Cr to reach the oxide surface. The dispersion of  $\text{Y}_2\text{O}_3$  may have contributed to scale formation by promoting a fine grain size in the matrix that increased the diffusion of Cr to the scale–metal interface.

## Acknowledgements

This research was supported by the US Department of Energy, Fossil Energy AR&TD Materials Program under contract DE-AC05-96OR22464 with Lockheed Martin Energy Research Corporation and the Oak Ridge National Laboratory (ORNL) Postdoctoral Research Associates Program administered jointly by ORNL and the Oak Ridge Institute for Science and Education.

## References

- [1] S. Ukai, T. Nishida, H. Okada, T. Okuda, M. Fujiwara, K. Asabe, *J. Nucl. Sci. Technol.* 34 (3) (1997) 256.
- [2] I.G. Wright, J.A. Calwell, D.R. Baer, J.T. Prater, L.H. Schoenlein, in: Effects of minor alloying additions on the formation of protective scales under sulfidizing conditions at  $700^\circ\text{C}$ , Report No. ORNL/Sub/86-57444/02, 1990.
- [3] A. Kumar, D.L. Douglass, *Oxid. Met.* 10 (1) (1976) 1.
- [4] S.N. Basu, D. Nath, J. Tebbets, in: H.A. Atwater (Ed.), Evolution of Surface and Thin Film Microstructures, *Mater. Res. Soc.*, 280, 1993, p. 541.
- [5] C.S. McDowell, S.N. Basu, *Oxid. Met.* 43 (3&4) (1995) 263.
- [6] R.C. Lobb, M.J. Bennett, *Oxid. Met.* 35 (1&2) (1991) 35.
- [7] M. Ahmad, K.A. Shoaib, M.A. Shaikh, K. Ehrlich, *J. Mater. Sci. Lett.* 14 (1995) 577.
- [8] M.P. Brady, B.A. Pint, P.F. Tortorelli, I.G. Wright, R.J. Hanrahan Jr, *Corros. Environ. Degrad. Mater.* 19 (1999) 1.
- [9] B.A. Pint, *Oxid. Met.* 45 (1&2) (1996) 1.
- [10] B.A. Pint, A.J. Garratt-Reed, L.W. Hobbs, *Mater. High Temp.* 13 (1) (1995) 3.